Topological susceptibility on dynamical staggered fermion configurations

Anna Hasenfratz*
Physics Department, University of Colorado, Boulder, Colorado 80309
(Received 2 May 2001; published 5 September 2001)

Topological susceptibility is one of the few physical quantities that directly measures the properties of the QCD vacuum. Chiral perturbation theory predicts that in the small quark mass limit the topological susceptibility depends quadratically on the pion mass, approaching zero in the chiral limit. Lattice calculations have difficulty reproducing this behavior. In this paper we study the topological susceptibility on dynamical staggered fermion configurations. Our results indicate that the lattice spacing has to be small, around $a \approx 0.1$ fm, for thin link staggered fermion actions to show the expected chiral behavior. Our preliminary result indicates that fat link fermions, on the other hand, reproduce the theoretical expectations even on lattices with $a \approx 0.17$ fm. We argue that this is due to the improved flavor symmetry of fat link fermionic actions.

DOI: 10.1103/PhysRevD.64.074503 PACS number(s): 11.15.Ha, 12.38.Aw, 12.38.Gc

I. INTRODUCTION

Instantons play an important role in the QCD vacuum from the breaking of the axial $U_A(1)$ symmetry to chiral symmetry breaking and the low energy hadron spectrum [1]. Lattice studies support many of the theoretical predictions [2]. For example, the Witten-Veneziano formula relates the pure gauge topological susceptibility to the masses of the η, η' and K mesons predicting $\chi_\infty^{1/4} = 180$ MeV. The topological susceptibility on pure gauge lattices has been measured by several groups using different methods, obtaining consistent results $\chi_\infty^{1/4} = 205(5)$ MeV [3–5].

Light fermions suppress the topological susceptibility. Chiral perturbation theory predicts [6]

$$\chi = \frac{m_q}{n_f}\Sigma + O(m_q^2) = \frac{f_\pi^2 m_\pi^2}{2n_f} + O(m_\pi^4), \tag{1}$$

where m_q is the quark mass, n_f is the number of fermion flavors, and Σ is the chiral condensate per fermionic flavor. In this normalization $f_\pi = 92$ MeV. Several recent lattice studies measured χ on dynamical configurations. Calculations with Wilson and clover fermions cover a fair range of lattice spacing $a \approx 0.08$–0.20 fm, and pion masses $m_\pi r_0 \approx 1.3$–2.5 (r_0 is the Sommer parameter [7]) [8–12]. The results appear controversial. UKQCD uses clover fermions [8–10]. Their data on lattices with $a \approx 0.1$ fm are basically consistent with Eq. (1). SESAM/TχL uses unimproved Wilson fermions. Their topological susceptibility at similar lattice spacing does not decrease with the pion mass though the statistical errors are too large to claim inconsistency with theoretical expectations [11]. CP-PACS published data using clover fermions and improved gauge action at lattice spacing $a \approx 0.17$ fm [12]. Their conclusion is the same as SESAM/$T\chi L$. The situation with staggered fermions is not much better. Only the Pisa group measured the topological susceptibility with two and four flavors of staggered fermions at lattice spacing $a \approx 0.09$–0.17 fm [13,14]. They do not see the reduction of the topological susceptibility with decreasing quark mass either.

Can we understand what is going on with the dynamical simulations? Equation (1) is valid only in the case of n_f light *chiral* fermions creating $n_f^2 - 1$ light pions. Both Wilson and staggered fermions violate this assumption. Wilson fermions break chiral symmetry explicitly. The addition of the clover term reduces the symmetry breaking and improves chiral behavior. Staggered fermions have only a residual $U(1)$ chiral symmetry and only one true Goldstone boson; the other pionlike states can be heavy. Fat link fermions considerably improve flavor symmetry and consequently chiral behavior. Both fermionic formulations should show the expected chiral behavior in the continuum limit, with clover and fat link fermions sooner than the unimproved ones, but it is not clear when scaling in the topological susceptibility actually sets in. In a recent paper [15] it was suggested that the reason the topological susceptibility from available lattice data does not follow the expected theoretical behavior is a combination of three effects: too large lattice spacing, too small volumes, and too small Leutwyler-Smilga [6] parameter. While all three conditions could indeed be important, we feel that the nonchiral behavior of the fermionic actions is the main cause of the problem. Chiral symmetry violation of the fermionic action is a scaling violation effect and is covered by the first condition of [15]. However, it is not a universal quantity, it can strongly depend on the fermionic action.

Why are the topological properties of the vacuum important? Phenomenological instanton models predict that the low energy hadron spectrum is governed by the near-zero eigenvalue modes of the Dirac operator which, in turn, are related to instantons. If the fermion-instanton interaction is different from the continuum one either because of chiral symmetry breaking or other lattice artifacts, the Dirac spectrum and consequently the low energy hadron spectrum can also be different. Recently, using chiral symmetric overlap fermions on the lattice, we showed that with light quarks the first few modes of the Dirac operator saturate the low lying hadron propagators on quenched $a \approx 0.12$ lattices, just as the phenomenological models predict [16,17]. In a subsequent

*Email address: anna@eotvos.colorado.edu

publication a contradictory conclusion was reached using Wilson fermions [18]. For us that implies that Wilson fermions, at least at large to moderate lattice spacings, interact differently with instantons than chirally symmetric fermions.

In this paper we investigate the topological susceptibility on both $n_f=2$ and $n_f=4$ staggered dynamical fermion configurations. The $n_f=2$ configurations are $16^3 32$ thin link staggered fermion lattices created by the Columbia and MILC Collaborations and downloaded from the NERSC archive [19]. The $n_f=4$ lattices are smaller; $8^3 24$ configurations used in the study of fat link fermions are in Ref. [20]. Two of the $n_f=4$ sets were generated with thin link staggered fermions and one with the $N=3$ level APE blocked fat link fermions [22,20]. The latter action has about an order of magnitude better flavor symmetry than thin link actions at similar parameter values. The thin link staggered fermion results with $a \leqslant 0.1$ fm are more or less consistent with Eq. (1). The thin link $a \approx 0.17$ fm data shows clear deviation, where the topological susceptibility is consistent with the quenched value, independent of the pion mass. On the other hand, the fat link data at the same coarse lattice spacing is in perfect agreement with Eq. (1), suggesting that improved flavor/chiral symmetry indeed has a strong effect on the topology.

To determine the topological charge of the configurations we used a topological charge density operator constructed from hypercubic blocked (HYP) fat links [21]. Hypercubic blocking was introduced in a recent paper as an alternative to repeated APE smearing [22]. Hypercubic blocking mixes links only from the hypercubes that attach to a given link, thus the fat link is very compact yet the configuration is as smooth as after three levels of APE blocking. To avoid the distortion effect of extended operators, we consider only one to three levels of hypercubic blocked operators (HYP1, HYP2, and HYP3). We have calculated the additive and multiplicative renormalization factors of the topological susceptibility for these operators. After two to three levels of HYP blocking the renormalization factors turn out to be consistent with their tree level values and, after correction, all three HYP topological susceptibility measurements are consistent.

In Sec. II we describe the hypercubic topological operator and illustrate the measurement of the renormalization factors on pure gauge Wilson plaquette configurations. Section III contains our results for two- and four-flavor staggered fermions. Section IV is a short discussion on flavor symmetry and the summary of our results.

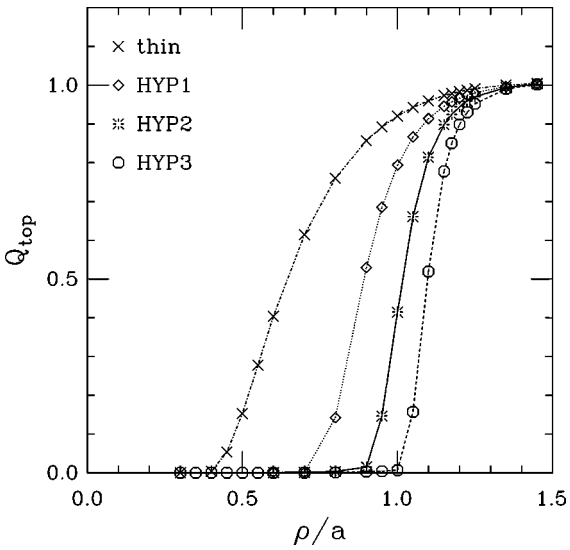

FIG. 1. The topological charge of a smooth instanton as the function of its radius ρ/a. The charge is measured with thin link operator (crosses), HYP1 (diamonds), HYP2 (bursts), and HYP3 (octagons) fat link operators.

II. HYPERCUBIC TOPOLOGICAL CHARGE OPERATOR

Most large scale simulations use pure gauge observables to measure the topological susceptibility with some discretized version of the continuum $F\tilde{F}$ as the lattice charge density operator $q_L(x)$. The relation between the continuum and lattice topological susceptibilities contains both a multiplicative and an additive renormalization factor. The lattice charge density operator is related to that of the continuum through a multiplicative renormalization factor

$$q_L(x) = Z a^2 q(x). \tag{2}$$

In addition the correlator of two topological density operators has an additive correction term as well due to the mixing of $q_L(x)$ with other lattice operators

$$q_L(x) q_L(0) = Z^2 a^4 q(x) q(0) + m(x), \tag{3}$$

thus the topological susceptibility on the lattice is

$$\chi_L = \int q(x) q(0) d^4x = Z^2 a^4 \chi + M, \tag{4}$$

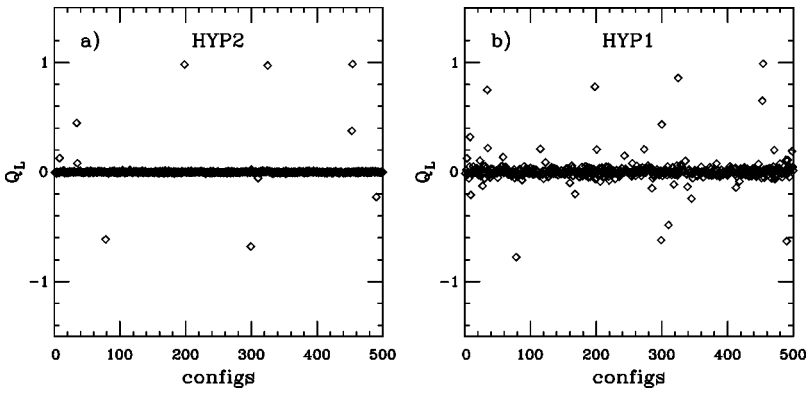

FIG. 2. The topological charge on 500 heated 8^4 $Q=0$ configurations measured with: (a) HYP2 topological operator, and (b) HYP1 topological operator. The configurations were heated with 10–50 heat bath steps using $\beta=6.0$ Wilson pure gauge action.

TABLE I. Results for the renormalization factors Z and M and the lattice and continuum topological susceptibilities for $\beta=6.0$ pure gauge Wilson action. The topological susceptibility was measured on 220 $16^3 32$ configurations downloaded from the NERSC archive [25].

	Z	$M\times10^5$	$\chi_L\times10^5$	$a^4\chi\times10^5$	χr_0^4
APE1	0.795(4)	0.95(7)	5.4(5)	7.0(7)	0.058(6)
HYP1	0.935(4)	0.11(3)	6.3(4)	7.1(5)	0.059(6)
HYP2	1.000(4)	0.006(4)	7.0(4)	7.0(4)	0.058(6)

$$M=\int m(x)d^4x. \tag{5}$$

The renormalization factors Z and M depend on the lattice parameters β and m_q. The renormalization constants in principle can be determined nonperturbatively using the heating method proposed by the Pisa group [23].

Because of lattice artifacts, (mainly dislocations), on typical lattices $Z\cong0.25$ and $M/\chi_L\cong1$ for thin link topological density operators, which makes the direct determination of χ almost impossible. Local smearing or cooling removes most of these lattice artifacts moving Z toward 1 and M toward 0. Repeated smoothing gives $Z\cong1$ and $M/\chi\ll1$ leading to $\chi_L\cong a^4\chi$. Since the nonperturbative calculation of Z and M introduces statistical and systematical errors, a topological density operator where the renormalization constants are small or can be neglected is desirable. However, repeated smearing and cooling methods have their drawbacks as well. While removing vacuum fluctuations and lattice artifacts, both methods remove topological objects, mainly small instantons and closeby pairs. In addition the size of the remaining objects changes as well, as can be demonstrated by monitoring individual instantons during the smearing process [3].

In this paper we construct the topological charge density operator $q_L(x)$ using hypercubic blocked links and the improved thin link charge operator of Refs. [24] and [3]. Hypercubic blocking was introduced in Ref. [21] as a localized alternative to repeated APE blocking. HYP fat links mix original links from the hypercubes that are attached to the fat link only, yet they create configurations that are as smooth as the ones obtained after three levels of APE blocking.

Topological charge measurements are difficult because of the presence of dislocations: short distance vacuum fluctuations that can be mistaken for small instantons. Smearing the links in the topological density operator reduces this problem in part by sharpening the transition between the topologically nontrivial $Q=\int d^4x q(x)=1$ sector and the trivial $Q=0$ sector. Figure 1 shows the topological charge of a smooth instanton measured with the thin link, HYP1, HYP2, and HYP3 fat link operators as the function of the instanton radius. The charge measured with the HYP operators rises sharply at instanton radius $\rho/a\approx1$.

Even though the HYP operators remove most dislocations, they still can have nontrivial renormalization factors. We have measured the renormalization factors Z and M following the heating method of Ref. [23]. To measure M one has to heat a trivial $Q=0$ configuration. The configuration thermalizes fast at short distances, and since the origin of M is in local contact terms, short distance thermalization is sufficient to measure M. Before heating creates nontrivial topological objects the thermalization must be terminated and restarted with a different random seed. It is important to make sure the measurement of M is done on $Q=0$ configurations only. Fortunately with the HYP3 and frequently with the HYP2 operators, it is easy to separate the trivial configurations from the occasional $Q\neq0$ ones. Figure 2(a) shows the topological charge on 500 heated $Q=0$ configurations measured with the HYP2 operator. Ordered 8^4 configurations were heated with 10–50 heat bath steps using $\beta=6.0$ pure gauge Wilson action. Most configurations have very small topological charge, a few have $|Q|\sim1$, and only 2–3 configurations have topological charge whose interpretation is not clear. I chose, based on Fig. 1 but somewhat arbitrarily, a cut $Q_{\max}=0.3$ to separate the $Q=0$ and $Q\neq0$ configurations. The final results are fairly insensitive to the precise choice of this cut. The topological charge measured with the HYP1 operator fluctuates more as is illustrated in Fig. 2(b). Again, a configuration is accepted as $Q=0$ if its topological charge is $|Q_L|<0.3$ as measured with the HYP2 operator. The multiplicative renormalization constant Z is calculated similarly on $Q=1$ configurations that contain a single smooth instanton of size $\rho/a=3.0$, 2.5, or 2.0. Z can be different on different instanton size backgrounds, although in any of the measurements we performed the difference was no more than a few percent. We chose Z on the background where the smooth instanton's size was closest to the expected average instanton size of the Monte Carlo configurations, $\rho/a\approx0.3$ fm/a.

Results for $\beta=6.0$ pure gauge Wilson action are summarized in Table I where Z, M, χ_L, $\chi a^4=(\chi_L-M)/Z^2$, and χr_0^4 with Sommer parameter $r_0=5.37(1)$ are given both for the HYP1 and HYP2 operator, and, for comparison, one level APE smeared operator with parameter $\alpha=0.75$ as well. The topological susceptibility was measured on 220 $16^3 32$ $\beta=6.0$ configurations from the NERSC archive [25]. The results for $a^4\chi$ are consistent for all three operators, in physical units $\chi^{1/4}=196(5)$ MeV. The renormalization factors, on the other hand, are quite different. The background term M is about 17% of χ_L for the APE1 operator, 2% for the HYP1 operator, and less than 0.1% for the HYP2 operator. The renormalization factors for the HYP2 operator are negligible, for all practical purposes we can use $Z=1$ and $M=0$.

Results are similar at $\beta=5.7$ although there one needs three levels of HYP blocking to reduce M to 0 and Z to 1 as

TABLE II. Results for the renormalization factors Z and M and the lattice and continuum topological susceptibilities for the $\beta=5.7$ pure gauge Wilson action. The topological susceptibility was measured on 350 $8^3 24$ configurations.

	Z	$M\times10^4$	$\chi_L\times10^4$	$a^4\chi\times10^4$	χr_0^4
HYP1	0.85(4)	0.6(1)	7.2(6)	9.1(16)	0.066(12)
HYP2	0.95(1)	0.19(4)	8.8(8)	9.5(12)	0.069(9)
HYP3	0.98(1)	0.02(1)	9.2(8)	9.4(11)	0.068(8)

TABLE III. Results for the topological susceptibility on $n_f=2$ configurations. All lattices are $16^3 32$ standard thin link staggered fermion configurations.

	$n_{\rm conf}$	r_0/a	a(fm)	am_π	$a^4\chi\times 10^5$	$(r_0 m_\pi)^2$	χr_0^4
$\beta=5.7$, $am_q=0.01$	83	6.29(8)	0.08	0.252(2)	2.6(3)	2.5(1)	0.041(6)
$\beta=5.7$, $am_q=0.015$	46	6.02(8)	0.08	0.293(2)	3.5(6)	3.1(1)	0.046(10)
$\beta=5.7$, $am_q=0.025$	33	5.8(1)	0.09	0.388(1)	5.8(9)	5.1(2)	0.065(15)
$\beta=5.415$, $am_q=0.025$	201	2.96(3)	0.17	0.4454(2)	84(8)	1.74(1)	0.064(9)

is illustrated in Table II. Here the topological susceptibility was measured on 350 $8^3 24$ lattices and the renormalization constants are obtained from 500 heated 8^4 lattices. The predictions for the continuum topological susceptibility are consistent from all three operators, $\chi^{1/4}=205(5)$ MeV. Within statistical errors it is also consistent, with the value obtained on the $\beta=6.0$ data set.

III. THE TOPOLOGICAL SUSCEPTIBILITY ON DYNAMICAL CONFIGURATIONS

A. Two flavors of staggered fermions

We have analyzed several two-flavor configuration sets using HYP1–HYP3 operators. The renormalization factors have to be calculated independently at every parameter value. The results for both Z and M were very similar to the quenched values at similar lattice spacing. We found that on configurations with lattice spacing $a\approx 0.1$ fm the renormalization constants of the HYP2 operator could be neglected, while with configurations with $a\approx 0.17$ fm the HYP2 operator had a few percent correction from the renormalization constants, and the HYP3 operator had none. Table III collects our results. All four data sets are from the NERSC archive: the first three were generated by the Columbia group, the last one by MILC [26,27]. All lattices are $16^2 32$ and use standard thin link staggered fermions with plaquette Wilson gauge action. am_π was measured in the original studies, r_0/a for the MILC lattice is from Ref. [28]. For the Columbia lattices we have measured r_0/a using HYP blocked Wilson loops. The HYP potential has greatly reduced statistical errors making it possible to obtain reliable values even from 33–83 configurations [21]. The lattice spacing in the fourth column was obtained using $r_0=0.5$ fm and is listed for future reference. Since the different HYP topological charge operators give consistent results, only the continuum value $a^4\chi$ is listed. The topological susceptibility for the first data set has been measured in Ref. [29] using 10–40 APE smeared operators. The values for $a^4\chi$ with APE smeared operators are consistent with the present result. In Fig. 3(a) χr_0^4 is plotted as the function of $(m_\pi r_0)^2$. The filled octagons correspond to the Columbia data sets with $a\leqslant 0.1$ fm. The filled diamond is the MILC lattice data with $a\approx 0.17$ fm. The filled square at the lowest $m_\pi r_0$ value is also from MILC. It is on a $24^3 64$, $\beta=5.6$, $am_q=0.01$ configuration set and was measured by DeTar using 10–20 level APE blocked topological operators [30]. The lattice spacing on these configurations is $a\approx 0.1$ fm, $r_0/a=4.99$. The dashed line in Fig. 3 is the leading order theoretical prediction from Eq. (1) using $f_\pi=92$ MeV. The three lowest $m_\pi r_0$ data points on the finer lattices with $a\leqslant 0.1$ fm are consistent, though a bit higher than the leading order theoretical curve. However, the data point with $a\approx 0.17$ fm is very different. The topological susceptibility on those lattices is consistent with the quenched result even though the pion mass is fairly small. Since on quenched configurations the topological susceptibility can be measured successfully even on coarse lattices, this discrepancy is not likely to be the consequence of the gauge system. Rather, it appears that the instantons do not feel the effect of light staggered fermions on coarse lattices. Flavor symmetry violation of staggered fermions can explain these findings. In Fig. 3(b) published Wilson/clover data are added to the $a\leqslant 0.1$ fm staggered data. Octagons correspond to the clover fermion simulations of UKQCD, are diamonds to the Wilson fermion simulations of SESAM/$T\chi L$. All Wilson/clover data has lattice spacing of $a\leqslant 0.1$ fm. The data from UKQCD are consistent with the staggered results and with the leading order theoretical curve as well. However the topological susceptibility with unimproved Wilson fermions does not follow the expected behavior at small pion mass. It remains large,

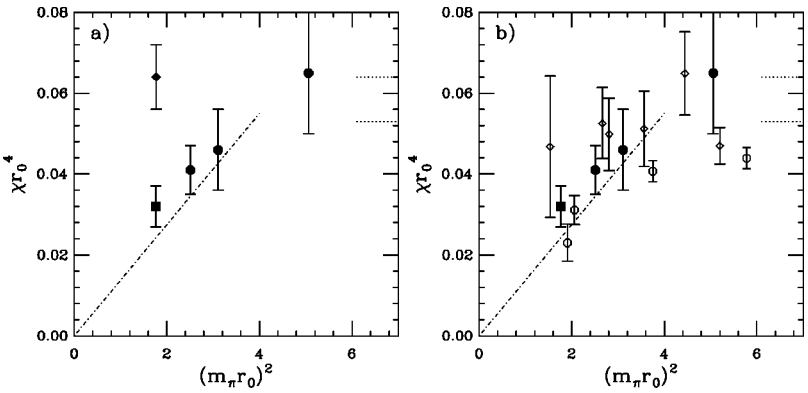

FIG. 3. χr_0^4 as the function of $(m_\pi r_0)^2$ with $n_f=2$ staggered fermions. The dashed line is the leading order theoretical prediction from Eq. (1) using $f_\pi=92$ MeV. The dotted lines on the right indicate the quenched value of χr_0^4. (a) Staggered fermions. Filled octagons: Columbia data sets; filled diamond: MILC data set; filled square: MILC [30]. (b) Same as (a) with Wilson/clover data added. Octagons: UKQCD; diamonds: SESAM/$T\chi L$.

TABLE IV. Results for the topological susceptibility on $n_f=4$ configurations. All lattices are $8^3 24$. The first two sets were generated with standard thin link staggered fermions, the third one with $N=3$ APE blocked fat link fermions.

	$n_{\rm conf}$	r_0/a	a(fm)	am_π	$a^4\chi\times 10^4$	$(r_0 m_\pi)^2$	χr_0^4
$\beta=5.2, am_q=0.06$, thin	188	2.85(2)	0.18	0.661(1)	8.5(9)	3.5(1)	0.056(8)
$\beta=5.25, am_q=0.06$, thin	189	3.48(3)	0.14	0.664(1)	4.8(5)	5.3(1)	0.070(10)
$\beta=5.2, am_q=0.1$, fat	140	2.97(3)	0.17	0.695(4)	3.5(4)	4.2(2)	0.026(4)

consistent with the quenched result, the same behavior we saw with staggered fermions at lattice spacing $a\approx 0.17$ fm. It appears that Wilson fermions have a very different effect on instantons even on finer, $a\approx 0.1$ fm lattices than clover or even unimproved staggered fermions. This is likely the consequence of chiral symmetry breaking of the Wilson action.

B. Four flavors of staggered fermions

Unfortunately we could not find any large $n_f=4$ staggered data sets to use. In Ref. [20], where we proposed a dynamical fat link fermion update, we generated three $8^3 24$ $n_f=4$ data sets to study flavor symmetry breaking of thin and fat link actions. The first two sets were generated with standard thin link staggered fermions, the third one with $N=3$ APE blocked fat link fermions. All three sets have lattice spacing $a\approx 0.17$ fm as shown in Table IV. The pion mass values in the table are also from Ref. [20] but we have reanalyzed the potential data using HYP Wilson loops and the r_0/a values listed in Table IV are more reliable and slightly different from the ones used in Ref. [20] The difference in the topological susceptibilities between the thin and fat link actions is striking. There is no Wilson/clover fermion data available at $n_f=4$ to compare the staggered result with. In Fig. 4 we plot χr_0^4 as the function of $(m_\pi r_0)^2$ for the three data sets from Table IV. The dashed line is the leading order theoretical prediction from Eq. (1) using the experimental value $f_\pi=92$ MeV. The fat link action data shows the expected behavior, while the thin link action topological susceptibility values are consistent with the quenched result, independent of the dynamical quark mass. For the thin link action this is the same behavior we saw with the $n_f=2$ data at similar lattice spacing.

IV. DISCUSSION AND SUMMARY

The interaction between light quarks and instantons changes the QCD vacuum substantially. One of the easiest way to get information about this effect is through the topological susceptibility that is expected to scale with the square of the pion mass in the small quark mass limit.

Our results indicate that thin link staggered fermions at lattice spacing $a\geqslant 0.17$ fm do not have the expected continuum effect on instantons, where a lattice spacing $a\approx 0.1$ fm is needed to recover the proper chiral behavior. In contrast to that, fat link staggered fermions show the expected behavior even on coarser $a\approx 0.17$ fm lattices. Can this be understood as the effect of flavor symmetry violation? In Refs. [20,21] we studied flavor symmetry violation on quenched lattices both with the thin link $N=3$ APE blocked and hypercubic blocked fat link fermions. The two fat link formulations have about the same level of flavor symmetry violations as measured by the relative mass splitting $\Delta_\pi=(m_\pi-m_G)/m_G$ between the Goldstone pion m_G and the other pionlike objects m_π. For thin link fermions at $(m_\pi r_0)^2\approx 2.0$ we found $\Delta_\pi\approx 0.7$ at $a\approx 0.17$ fm, and $\Delta_\pi\approx 0.2$ at $a\approx 0.1$ fm for the lightest non-Goldstone pions. The corresponding values for fat link fermions are $\Delta_\pi\approx 0.09$ and $\Delta_\pi\approx 0.01$, respectively. QCD with two(four) light flavors should have 3(15) light pions. Apparently when there is only one light pion and the other pion-like objects are 70% or more heavier than the Goldstone pion, the vacuum does not look like a two- (four)-flavor QCD vacuum. The flavor symmetry breaking has to be reduced below 20% to get acceptable results. Fat link fermions can do that easily even on coarse lattices.

Available lattice data for Wilson/cover fermions can be understood similarly. The topological susceptibility with clover fermions is consistent with the theoretical predictions at lattice spacing $a\approx 0.1$ fm but the Wilson fermion data at the same lattice spacing indicate that unimproved Wilson fermions, which have much larger chiral symmetry violations, do

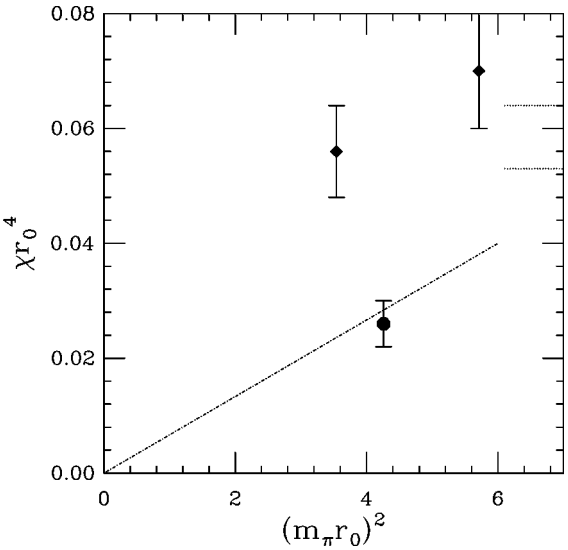

FIG. 4. χr_0^4 as the function of $(m_\pi r_0)^2$ with $n_f=4$ staggered fermions. The filled diamonds are from thin link staggered configurations; the filled octagon is from fat link dynamical configurations. The dashed line is the leading order theoretical prediction from Eq. (1) using the experimental value $f_\pi=92$ MeV. The dotted lines on the right indicate the quenched value of χr_0^4.

not have the expected continuum-like interaction even at $a \approx 0.1$ fm. Results from CP-PACS at lattice spacing $a \approx 0.17$ fm indicate that at that lattice spacing not even clover fermions can reproduce the continuum topological behavior. Fat link clover fermions improve chiral symmetry and could provide a better alternative to thin link clover fermions. It would be interesting to find a parameter similar to Δ_π that correlates with the level of chiral symmetry breaking for the Wilson-like fermions and compare it with the topological susceptibility.

One should be concerned about dynamical simulations where the topological susceptibility is not reproduced correctly, since that indicates that the vacuum at those simulations is more like the quenched vacuum rather than the expected dynamical one. Improving chiral symmetry can have a profound effect. This point is further underscored in a forthcoming publication about the finite temperature phase diagram obtained with fat link fermions [31].

ACKNOWLEDGMENTS

This work was largely inspired by collaboration with F. Knechtli on fat link fermions and hypercubic blocking. G. Bali convinced me that in order to compare the topological susceptibilities from different simulations one needs to use a reliable scale, such as r_0. That prompted the potential measurements with hypercubic blocked links. S. Gottlieb helped me out with some of the MILC staggered fermion data. The numerical calculations of this work were performed on the Colorado-HEP α cluster.

[1] T. Schafer and E.V. Shuryak, Rev. Mod. Phys. **70**, 323 (1998).
[2] M.G. Perez, Nucl. Phys. B (Proc. Suppl.) **94**, 27 (2001).
[3] A. Hasenfratz and C. Nieter, Phys. Lett. B **439**, 366 (1998).
[4] P. de Forcrand, M.G. Perez, J.E. Hetrick, and I.-O. Stamatescu, Nucl. Phys. B (Proc. Suppl.) **63**, 549 (1998).
[5] B. Alles, M. D'Elia, and A.D. Giacomo, Nucl. Phys. **B494**, 281 (1997).
[6] H. Leutwyler and A. Smilga, Phys. Rev. D **46**, 5607 (1992).
[7] R. Sommer, Nucl. Phys. **B411**, 839 (1994).
[8] A. Hart and M. Teper, Nucl. Phys. B (Proc. Suppl.) **83**, 476 (2000).
[9] UKQCD Collaboration, A. Hart and M. Teper hep-lat/0009008.
[10] UKQCD Collaboration, A. Hart and M. Teper hep-ph/0004180.
[11] SESAM Collaboration, G.S. Bali *et al.*, Phys. Rev. D (to be published) hep-lat/0102002.
[12] CP-PACS Collaboration, A.A. Khan *et al.*, Nucl. Phys. B (Proc. Suppl.) **83**, 162 (2000).
[13] B. Alles, M. D'Elia, and A.D. Giacomo, Phys. Lett. B **483**, 139 (2000).
[14] B. Alles, M. D'Elia, and A.D. Giacomo, Nucl. Phys. B (Proc. Suppl.) **83**, 431 (2000).
[15] S. Durr, hep-lat/0103011.
[16] T. DeGrand and A. Hasenfratz, Phys. Rev. D **64**, 034512 (2001).
[17] T. DeGrand and A. Hasenfratz, hep-lat/0103002.
[18] I. Horvath, N. Isgur, J. McCune, and H.B. Thacker hep-lat/0102003.
[19] NERSC Gauge Connection, http://qcd.nersc.gov/.
[20] F. Knechtli and A. Hasenfratz, Phys. Rev. D **63**, 114502 (2001).
[21] A. Hasenfratz and F. Knechtli, Phys. Rev. D **64**, 034504 (2001).
[22] APE Collaboration, M. Albanese *et al.*, Phys. Lett. B **192**, 163 (1987).
[23] C. Christou, A.D. Giacomo, H. Panagopoulos, and E. Vicari, Phys. Rev. D **53**, 2619 (1996).
[24] T. DeGrand, A. Hasenfratz, and T.G. Kovacs Nucl. Phys. **B520**, 301 (1998).
[25] G. Kilcup, D. Pekurovsky, and L. Venkataraman, Nucl. Phys. B (Proc. Suppl.) **53**, 345 (1997).
[26] F.R. Brown *et al.*, Phys. Rev. Lett. **67**, 1062 (1991).
[27] MILC Collaboration, C. Bernard *et al.*, Nucl. Phys. B (Proc. Suppl.) **73**, 198 (1999).
[28] S. Tamhankar and S. Gottlieb, Nucl. Phys. B (Proc. Suppl.) **83**, 212 (2000).
[29] A. Hasenfratz, Phys. Lett. B **476**, 188 (2000).
[30] C. DeTar (private communication).
[31] A. Hasenfratz and F. Knechtli, hep-lat/0105022.